DESIGN OF A FOUR-POINT BEND TEST FOR ULTRA-LOW CYCLE FATIGUE OF PIPELINES UNDER INELASTIC BENDING

T. Muylaert[1] and W. De Waele[1]

[1] Ghent University, Laboratory Soete, Belgium

Abstract This master thesis is situated in the research domain dealing with the ductile failure of pipelines under extreme loading conditions. It is part of an umbrella research aiming to develop innovative experimental and computational methodologies to simulate fracture of steel structural elements under ultra-low cycle fatigue. The focus of this study is on steel pipeline applications. The objective of this thesis is to design a large-scale four-point bend test setup to cyclically bend pipes. The feasibility of instrumentation will be evaluated using small scale test specimens. In this paper some ideas, constraints and opportunities for the design are considered, based on a literature review of several test setups for other applications. The design parameters have been calculated to compose the design windows and an initial overview of the possible instrumentation is given.

Keywords: pipe; four-point bending; ultra-low cycle fatigue; inelastic;

1 INTRODUCTION

The oil and gas industry is developing very quickly. The demand for high operating pressure, long distance and large diameter pipelines leads to the use of high strength steels exposed to extreme loading conditions. Especially in areas susceptible to earthquakes, in reel pipe laying and in offshore structures. Under these conditions, repeated and extended deformations into the plastic range must be survived. The pipeline design has to take into account the ductile failure mode of steel under ultra low cycle fatigue conditions.

The purpose of this thesis is the design and instrumentation of a large-scale four-point bend test setup to simulate ultra-low cycle fatigue (ULCF) of pipes. Pipes will be exposed to inelastic bending and internal pressure. On the long term, experimental results will serve to calibrate and optimize simulation models and to develop design guidelines for strain based ULCF design.

Conventional stress-based design limits the allowable stress by applying a design factor on the specified minimum yield strength (SMYS). However, stress-based design will be insufficient in cases where displacement-controlled loads are the dominant design conditions [1]. Because of ecological, economical and safety reasons, there is a need for adequate strain-based design tools.

Strain-based design is applied in two areas: structures subjected to static loads, and structures subjected to loads varying with time. These loading conditions may lead to monotonic ductile fractures or to ULCF (number of cycles to failure N_f in the order of 10^2). The micro-mechanisms that determine failure in ULCF (void nucleation, growth and coalescence) are different from those in low cycle fatigue (N_f ~10^3) (See Figure 1 and Figure 2 [2, 3]). These micro-mechanisms in ULCF are not yet fully understood and characterised.

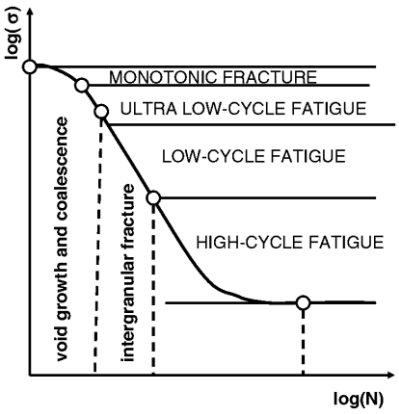

Figure 1. Definition of failure mechanism as a function of number of cycles [2]

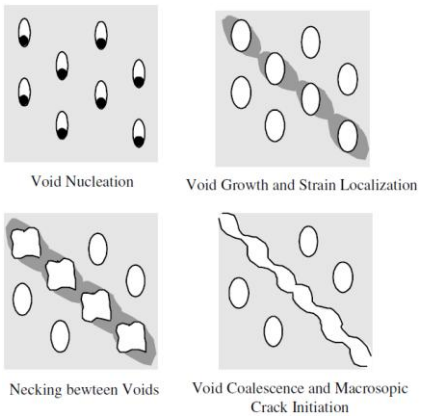

Figure 2. Micromechanical process of ductile fracture in steel [3]

In literature a lot of test results are reported, obtained from the monotonic bending of pipelines [4-8], the monotonic buckling behaviour of pipelines [7, 9, 10], and the wrinkling of tubes by axial cycling [11, 12]. There is also a lot of research effort to asses possible fracture due to an initial flaw in limited yielding (J-integral, Crack Opening Displacement) [7, 9]. However, research on pipes subjected to inelastic bending

together with ULCF is rare [13-16]. No test setups of this size for inelastic reverse four-point bending were found in literature.

Pioneering research on inelastic cyclic bending of tubes was carried out by Shaw, Kyriakides and Corona [4, 5, 12, 15-19] on small tubes (Ø 31.7mm). They cycled the tubes in a range of curvatures less than the critical one in monotonic bending.

2 DESIGN CONCEPT

2.1 Literature review of pipe bending setups

The cyclic bending machine for tubes designed by Kyriakides is shown in Figure 3 [14].

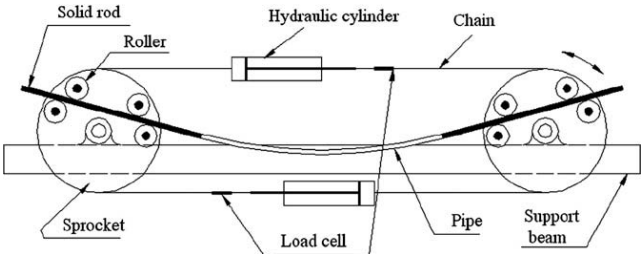

Figure 3. Cyclic plastic bending machine of Kyriakides, Shaw and Corona [14]

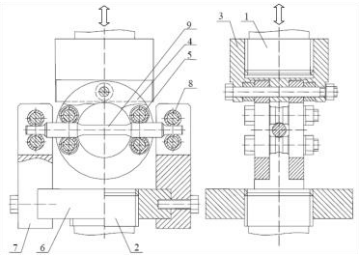

Figure 4. Cyclic elastic-plastic bending test setup at Laboratory of Kaunas University of Technology [20]

This is a very suitable design to test tubes in ULCF conditions. Unfortunately, for large pipes this concept would be almost impossible nor safe enough (chain can accumulate high elastic energy which can be suddenly released in case of failure [1]). Another interesting design to cyclically bend small circular cross-section elements is shown in Figure 4 [20]. Both test setups introduce forces by supporting rollers. Because of the size of the desired setup, this would initiate local stress concentration and accelerate local buckling.

For large scale tests, inspiration was found in several monotonic bending test setups reported in literature (see Figure 5 to Figure 8 [1, 10, 21, 22]). These designs can only bend in one direction and were typically developed for the evaluation of buckling or monotonic ductile fracture, which is not the purpose of this research. Nevertheless, instrumentation, methodologies, load and displacement values and results can be compared. In Figure 9 [23] a four point bending test setup is shown that has been used to investigate bending fatigue in the elastic range.

A critical part of the setup is the load introduction on the pipe specimen. The clamping must allow ovalization, longitudinal displacement, rotation and must ensure even load introduction, thus avoiding local stress concentrations. If the bending is only in one direction, this can easily be done with metal straps (see Figure 5 [22]). Several concepts applicable for cyclic bending have been considered.

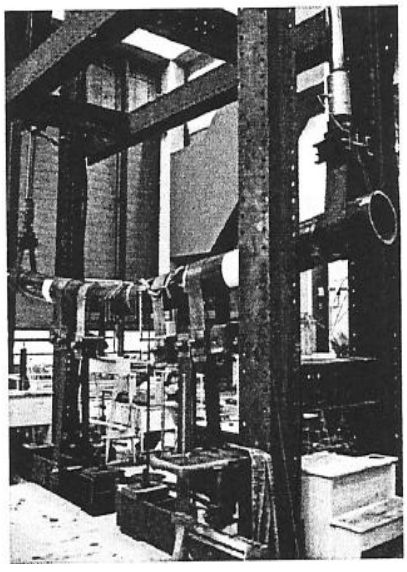

Figure 5. Monotonic plastic four-point bend test rig at TU Delft [22]

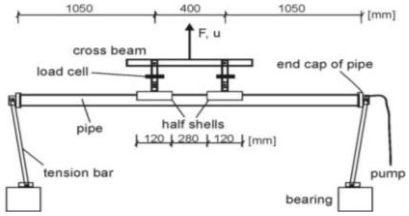

Figure 6. Monotonic elastic-plastic four-point bend test setup at Hannover University [10]

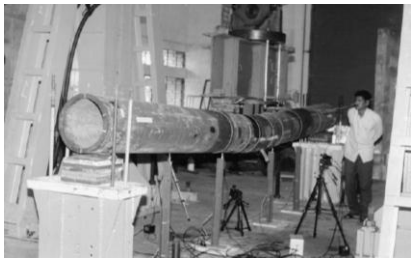

Figure 7. Monotonic plastic pipe fracture test setup at Bhabha Atomic Research Centre, Mumbai [21]

Figure 8. Monotonic plastic full-scale bending on CSM test rig by CSM and University of Cagliari [1]

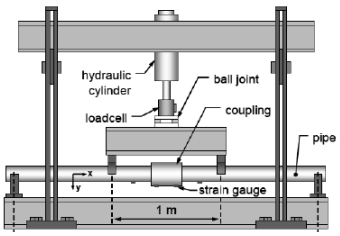

Figure 9. Elastic fatigue four-point bend test setup of Laboratory Soete, Ghent University [23]

Table 1. Properties of bending setups

	Figure 3	Figure 4	Figure 5	Figure 6	Figure 7	Figure 8	Figure 9	Figure 10	Current design
Cylinder(s) capacity (kN)		50	2*800	> 450	1000	2*8000			ca 1000
Stroke (mm)			1500	>100	250	15000			250 - 400
Pipe diameter (mm)	32 - 35	12	305	66,1	200 / 400	508 - 1420	25,4	125	219 - 508
D/t	15 - 45	solid		132	12,6 / 14,5	64,5			17,25 - 80
Inner span (mm)		66	1600	400	1480	5000 - 12000	1000	955	1500
Outer span (mm)	1250	140	6000	2500	4000 / 5820	32000	3000	2615	6000
Cyclic/Monotonic	cy	cy	mo	mo	mo	mo	cy	cy	cy
Elastic/Plastic	pl	el	pl	pl	pl	pl	el	pl	pl

2.2 Design concept

The aim of this study is to develop a design for testing of pipes in ULCF conditions. A test setup design was proposed (see Figure 10). However, there can be a problem with horizontal forces working on the load cell and cylinder. The rotating support induces a secondary bending load which causes a maximum moment in the middle pipe section [1]. This can be taken into account, or a solution could be found in a double hinge or a moving hinge (see Figure 6 and Figure 8 [1, 10]). The latter is the best option because a double hinge gives problems with testing in both directions. To protect the hydraulic cylinder against momentum and horizontal forces, a vertical guidance could be installed alongside the cylinder. Disadvantages are the voluminous design and unwanted friction force influencing the load cell. For these reasons, it is chosen to install LVDT's on the cylinder to signal horizontal displacement and stop the test if necessary.

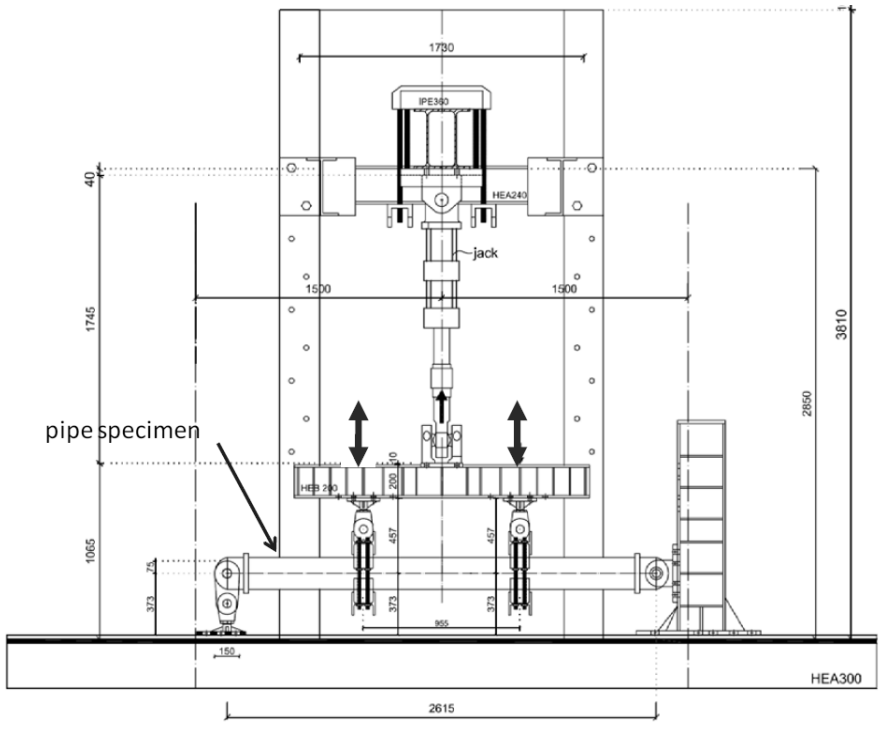

Figure 10. ULCF four-point bending test concept

Tests can be performed in displacement or in load control. When the pipe reaches its maximum static moment capacity, an increase in moment (load controlled) would result in rapid failure. However, in the proposed test setup the maximum static moment capacity will not be reached (see Figure 14). Because of safety reasons and because higher curvatures can be reached, the tests will be displacement controlled.

To reduce the susceptibility to local buckling, internal pressure can be applied. This induces a load controlled tensile hoop stress which postpones the onset of buckling [10, 24].

3 DESIGN CALCULATIONS

In preparation of the detailed design, some design parameters need to be calculated. Two key parameters are the force *F* and the stroke *u* of the cylinder.

3.1 Force and moment

Calculation of the elastic and plastic bending moments (respectively M_e and M_{pl}) is based on the formulae for the elastic [25] and plastic section modulus [26], W_{el} and W_{pl} respectively.

The elastic moment is calculated as follows.

$$W_{el} = \pi \frac{D_{out}^4 - D_{in}^4}{32 D_{out}} \tag{1}$$

$$M_{el} = FS.W_{el} \tag{2}$$

In these equations D_{out} and D_{in} are respectively the outer and inner pipe diameter (in mm).

Strain hardening is taken into account through calculation with the flow stress *FS* (MPa), defined as the average of the yield strength and the tensile strength values [27].

The fully plastic moment M_{pl} is calculated as follows.

$$W_{pl} = \frac{D_{out}^3 - D_{in}^3}{6} \tag{3}$$

$$M_{pl} = FS.W_{pl} \tag{4}$$

A more advanced calculation method is needed to take partial plastification of the cross section into account. Calculation of the elastic-plastic bending moment in function of the plastic section β (See Figure 11 [28]) is described in [28] for a solid rectangular cross section. These formulas have been adjusted to calculate the bending moment of a tubular cross section. The bending moment is then calculated as given in Eq. (7).

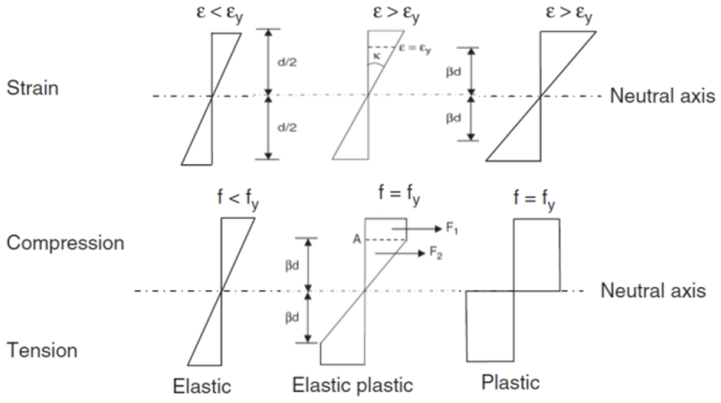

Figure 11. Plastification of a cross section
(start yielding: β = 0,5; 45°: β = 0,46; fully plastic: β = 0) [28]

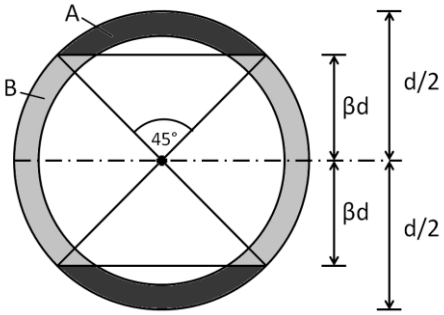

Figure 12. Plastic area (A) of a tubular cross section

The calculation of the elastic moment, the fully plastic moment and the elastic-plastic moment for a plastically deformed section of 45° (β=0,46) were performed in Maple as follows.

$$F_1 = FS.Area_A \tag{5}$$

$$F_2 = \frac{Centroid_B}{\beta.D_{out}} FS.Area_B \tag{6}$$

$$M_\beta = 2\left(F_1.Centroid_A + F_2.Centroid_{F2}\right) \tag{7}$$

$$F_{applied} = 2\frac{M}{a} \tag{8}$$

In these equations F_1 is the axial force in $area_A$, F_2 the axial force in $area_B$, βD the distance from the neutral axis at which yielding starts, $centroid_A$ the center of mass of $area_A$, $centroid_{F2}$ the center of mass of $area_B$ combined with the point of application of F_2 (see Figure 11 and Figure 12). M and $F_{applied}$ are respectively the total applied moment and force, a is the distance from inner to outer clamping.

3.2 Curvature and displacement

The moment-curvature relation during elastic-plastic bending can be found in [29] (see Figure 13 and Figure 14 [7]).

$$m = \frac{2}{\pi}\left[\varphi.\arcsin\frac{1}{\varphi} + \sqrt{1-\frac{1}{\varphi^2}}\right] \tag{9}$$

With $m = M/M_{el}$ and $\varphi = \kappa/\kappa_{el}$ in which κ is the curvature.

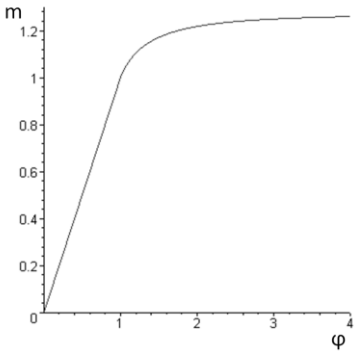

Figure 13. Moment-curvature relation during elastic-plastic bending

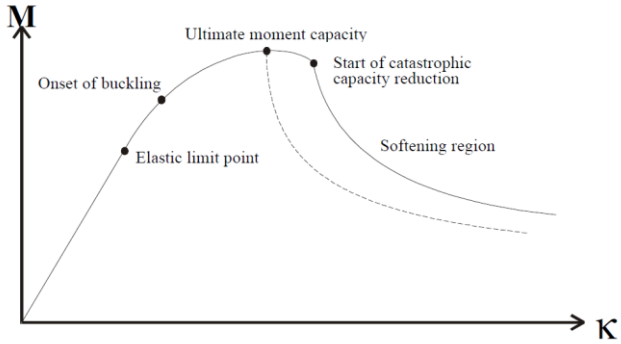

Figure 14 Examples of bending moment versus curvature relation [7]

This function is applicable for an elastic-perfectly plastic material. In reality, due to strain hardening, the load will slightly increase at rapidly increasing deflection when the beam is loaded beyond its theoretical collapse load [28]. In this theoretical approach the curvature goes to infinity as the ratio m approaches 1,273; the shape factor of a tube.

For design purposes the elastic curvature is calculated based on the flow stress. This gives an over-estimation of the expected elastic displacement.

$$\kappa_{el} = \frac{2FS}{E.D_{out}} \tag{10}$$

$$\kappa_{\beta} = \varphi.\kappa_{el} \tag{11}$$

For simplicity, the calculated elastic-plastic curvature κ is assumed constant for the inner span, which gives an over-estimation of the displacement. The displacement of the outer span is calculated with the elastic theory.

3.3 Comparison with critical buckling strains reported in literature

In literature different methods are used to estimate the critical buckling strain. In an ULCF test the critical strain should not be reached, but it can be used as reference. In this section, the inner span (i.e. the region between the load introduction points) is curved with the calculated plastic curvature, the outer span is calculated with the elastic curvature. In [30] several design formulae are found to calculate the critical strain and corresponding moment. The most conservative critical moment is described in BS8010 (1993), Eq. (12).

$$M_c = M_p\left(1 - 0{,}0024\frac{D_{out}}{t_{nom}}\right) \tag{12}$$

$$M_p = \left(D_{out} - t_{nom}\right)^2 t_{nom}\sigma_y \tag{13}$$

For the critical strain, the most conservative (BS8010 Eq. (14)), the most recent (ABS (2001) Eq. (16)) and an intermediate formula (Gresnigt Eq. (16) [10]) are applied to plot the critical stroke in the design window (see Figure 15).

$$\varepsilon_{cr} = 15\left(\frac{t_{nom}}{D_{out}}\right)^2 \tag{14}$$

$$\varepsilon_{cr} = 0{,}5\frac{t}{D_{out}} \tag{15}$$

$$\varepsilon_{cr} = 0{,}25\frac{t}{D_{out}/2} - 0{,}0025 \tag{16}$$

The fatigue life in ULCF can be roughly estimated with Eq. (17) [31]. This formula is fitted to experiments for R = 0, but it has been reported that in ULCF the effect of the mean stress is negligible. Due to missing data for an API 5L grade X80 pipeline, the material constants for annealed 1018 Carbon steel, λ=1,05 and k=0,5, have been applied. These material constants are probably not adequate for an X80 pipeline, nevertheless it gives an idea of the order of magnitude.

$$N_f = \frac{1}{2}\frac{e^{\lambda} - 1}{e^{\lambda\left(\frac{\varepsilon_d}{\varepsilon_f}\right)^{1/k}} - 1} \tag{17}$$

With ε_f the fracture strain and ε_d the plastic distortion. For an API 5L grade X80 pipeline it is assumed that ε_f = 0,18 and the applied ε_d ranges from 0,02 to 0,08 giving a theoretical life N_f in the order of respectively 70 to 4 cycles.

3.3 Design windows

The necessary force and displacement are calculated for several diameters (8 – 20”) and thicknesses (5,6 – 12,7 mm) which results in the design window shown in Figure 15. Based hereon a hydraulic cylinder can be chosen.

To avoid buckling, the critical load displayed (cross) should never be reached during the test. For low *D/t*-ratios, the critical values for the force are clearly between a 45° plastic and a fully plastic section. For higher values of *D/t*, the critical value will be reached before a section of 45° is yielding or the applied formulae are outside their application range (i.e. the critical value for buckling is reached before the onset of yielding).

The critical stroke to avoid buckling becomes excessively high for low *D/t*-ratios. It means that for this *D/t*-ratio buckling is not likely to happen, but rather localised ovalization or fracture. For higher *D/t*-ratios, the calculated values for a 45° plastic zone and the critical values come closer, so buckling is more likely to happen.

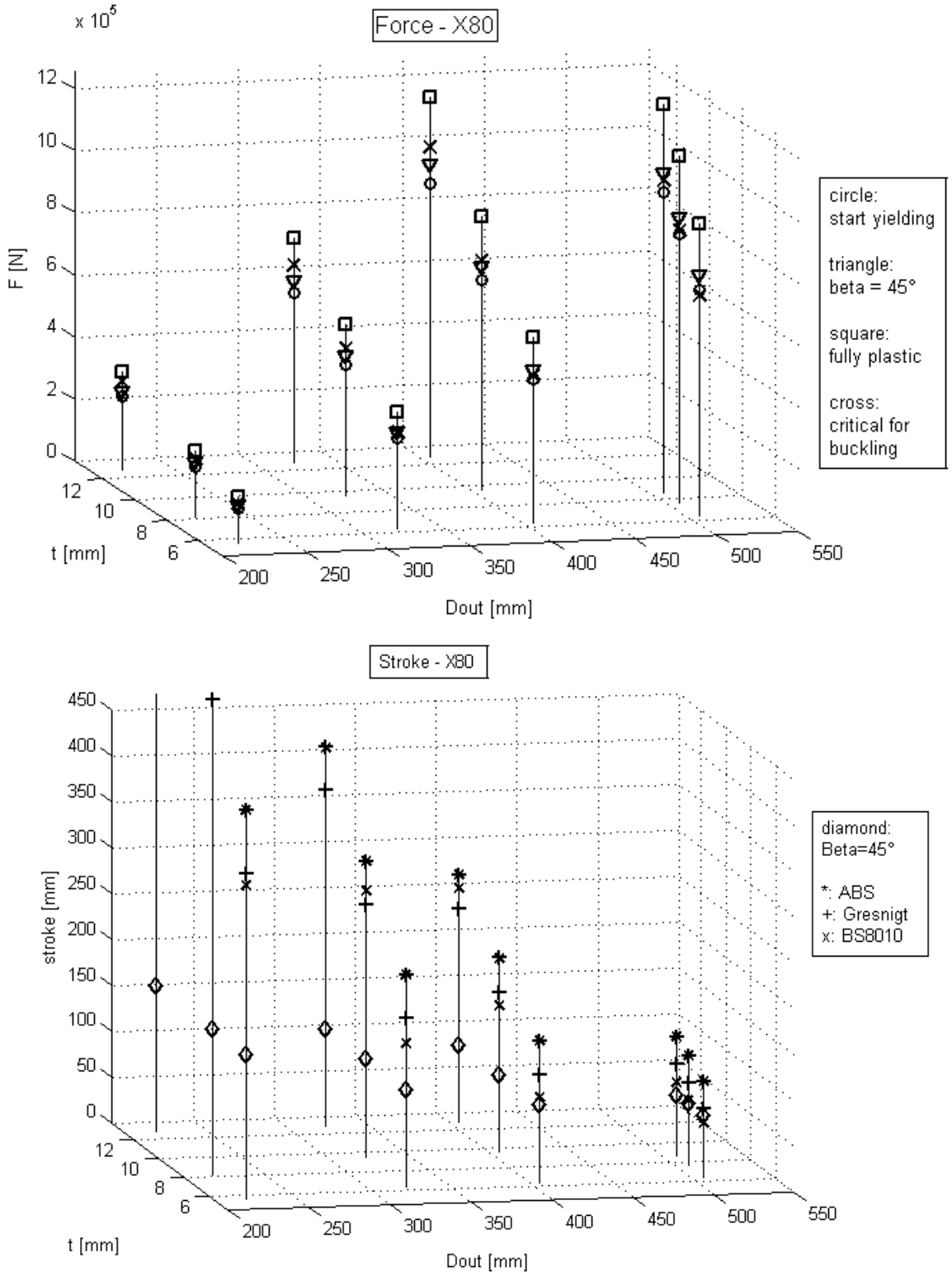

Figure 15. Design windows: force and stroke (for β=45°) as a function of the thickness and the outer diameter of the pipe

4 INSTRUMENTATION

The full scale tests require proper instrumentation in order to measure local quantities for a detailed comparison with FE models (local strains, plasticity and fracture initiation). Comparison will be also performed on global quantities (e.g. load vs. stroke curves) in order to validate the geometrical and stiffness correctness of the FE models (elastic behaviour, widespread plasticity after first yielding, elastic-plastic response after cycling).

A short overview of the possible instrumentation which will be considered is shown in Table 2.

Table 2. Overview of possible instrumentation

Measured quantity	NAME	RESULT	ANNOTATIONS	REAL TIME	REF.
GLOBAL					
Load	Load cell	Vertical force	Moment sensitivity errors	Yes	
Stroke	LVDT	Displacement	Displacement control	Yes	
Curvature	PONTOS: Optical 3D displacement measuring system	Position, movement and deformation		No	
	Curvature meter	Curvature	Backup for PONTOS	Yes	[22, 32]
	Cable extension position transducers	Displacement	Backup for PONTOS	Yes	
	Inclinometers	Angle	Can be derived from stroke	Yes	
LOCAL					
Strain	Digital image correlation	Deformation distribution (3D) Surface profile (3D) Strain distribution	Area of interest? ➔ FE? How to determine fracture initiation? ➔ macroscopic reading Possible on full pipe? ➔ small scale test	No	
	Strain gages	Strain	At critical locations After plastic instability the measurements could become worthless & misleading	Yes	[33]
Plasticity and fracture initiation	Macroscopic reading	Localize fracture	Smooth surface	Yes	
	Brittle coating to visualize deformation band clusters	Shatters at ± 1% strain	Must be cured at 49°C for 24h on test setup	Yes	[5]
Ovalization	Ovalization meter	ΔD		Yes	[15]
Temperature	Thermocouple	Temperature	Temperature does increase due to plastic deformation. Material properties do not significantly change with temperature	Yes	[3]
BEFORE	Material properties, Ovalization	True stress-strain curve, initial imperfections, etc.			
AFTER	Post fracture analysis	Fracture analysis			[23]

Further research must be performed to select the most appropriate instrumentation. The instrumentation will be evaluated in advance on a small scale test setup.

5 CONCLUSIONS

In the first part of this master thesis, a broad and deep literature review was performed on the design, material behaviour, instrumentation and test procedures. Some initial ideas, constraints and opportunities for the design have been determined. More research work has to be performed to come to a final design of the test setup. In this master thesis, the final design should be completed and some small scale tests will be executed to evaluate the instrumentation.

6 NOMENCLATURE

a	distance inner to outer clamping	mm
b	inner span	mm
W_{el}	elastic section modulus	mm³
W_{pl}	plastic section modulus	mm³
D_{out}	outer diameter	mm
D_{in}	inner diameter	mm
FS	flow strength	MPa
M_{el}	elastic moment	Nmm
M_{pl}	plastic moment	Nmm
β	indicates plastic area	-
M_{β}	moment for a plastic section β	Nmm
F	force	N
m	M/M_{el}	-
φ	κ/κ_{el}	-
κ	curvature	mm^{-1}
σ_y	yield strength	MPa
ε_{cr}	critical buckling strain	mm
N_f	number of life cycles	-
ε_f	fracture strain	mm
ε_d	plastic distortion	mm
λ	damage parameter	-
k	material constant	-

7 ACKNOWLEDGEMENTS

The discussions and advice of the Labo Soete personnel is greatly appreciated.

8 REFERENCES

1. Flaxa, V.e.a., *Full Scale Investigation On Strain Capacity Of High Grade Large Diameter Pipes.* 18th JTM, San Francisco CA, 2011.
2. Bleck, W., et al., *Numerical and experimental analyses of damage behaviour of steel moment connection.* Engineering Fracture Mechanics, 2009. **76**(10): p. 1531-1547.
3. Fell, B.V., *Large-Scale Testing and Simulation of Earthquake-Induced Ultra Low Cycle Fatigue in bracing members subjected to cyclic inelastic buckling*, 2008, University of California. p. 281.
4. Limam, A., et al., *Inelastic wrinkling and collapse of tubes under combined bending and internal pressure.* International Journal of Mechanical Sciences, 2010. **52**(5): p. 637-647.
5. Hallai, J.F. and S. Kyriakides, *On the effect of Lüders bands on the bending of steel tubes. Part I: Experiments.* International Journal of Solids and Structures, 2011. **48**(24): p. 3275-3284.
6. Ahn, S., et al., *Comparison of experimental and finite element analytical results for the strength and the deformation of pipes with local wall thinning subjected to bending moment.* Nuclear Engineering and Design, 2006. **236**(2): p. 140-155.
7. Hauch, S. and Y. Bai, *Bending moment capacity of groove corroded pipes.* Proceedings of the 10th (2000) International Offshore and Polar Engineering Conference, Vol Ii, 2000: p. 253-262.
8. Netto, T.A. and S.F. Estefen, *Ultimate strength behaviour of submarine pipelines under external pressure and bending.* J. Construct. Steel Research, 1994. **28**: p. 137-151.
9. Poursaeidi, E., G.H. Rahimi, and A.H. Vafai, *Plastic buckling of cylindrical shells with cutouts.* Asian journal of civil engineering (Building and Housing), 2004. **5**: p. 191-207.

10. Schaumann, P., C. Keindorf, and H. Bruggemann, *Elasto-plastic behavior and buckling analysis of steel pipelines exposed to internal pressure and addisional loads*, in *24th International Conference on Offshore Mechanics and Arctic Engineering*, 2005: Halkidiki, Greece.
11. Das, S., J.J.R. Cheng, and D.W. Murray, *Behavior of wrinkled steel pipelines subjected to cyclic axial loadings.* Canadian Journal of Civil Engineering, 2007. **34**(5): p. 598-607.
12. Jiao, R. and S. Kyriakides, *Wrinkling of Tubes by Axial Cycling.* Journal of Applied Mechanics, 2010. **77**(3): p. 031012.
13. Zhong, Y., et al., *Effect of toughness on low cycle fatigue behavior of pipeline steels.* Materials Letters, 2005. **59**(14-15): p. 1780-1784.
14. Chang, K. and W. Pan, *Buckling life estimation of circular tubes under cyclic bending.* International Journal of Solids and Structures, 2009. **46**(2): p. 254-270.
15. Kyriakides, S. and P.K. Shaw, *Inelastic Buckling Of Tubes under Cyclic Bending.* Journal of Pressure Vessel Technology-Transactions of the Asme, 1987. **109**(2): p. 169-178.
16. Shaw, P.K. and S. Kyriakides, *Inelastic Analysis of Thin-Walled Tubes under Cyclic Bending.* International Journal of Solids and Structures, 1985. **21**(11): p. 1073-1100.
17. Corona, E. and S. Kyriakides, *An Experimental Investigation of the Degradation and Buckling of Circular Tubes Under Cyclic Bending and External Pressure.* Thin-Walled Structures, 1991. **12**: p. 229-263.
18. Corona, E. and S. Kyriakides, *On the Collapse of Inelastic Tubes under Combined Bending and Pressure.* International Journal of Solids and Structures, 1988. **24**(5): p. 505-&.
19. Rahman, S.M., T. Hassan, and E. Corona, *Evaluation of cyclic plasticity models in ratcheting simulation of straight pipes under cyclic bending and steady internal pressure.* International Journal of Plasticity, 2008. **24**(10): p. 1756-1791.
20. Daunys, M. and S. Rimovskis, *Analysis of circular cross-section element, loaded by static and cyclic elastic–plastic pure bending.* International Journal of Fatigue, 2006. **28**(3): p. 211-222.
21. Chattopadhyay, J., H. Kushwaha, and E. Roos, *Some recent developments on integrity assessment of pipes and elbows. Part II: Experimental investigations.* International Journal of Solids and Structures, 2006. **43**(10): p. 2932-2958.
22. Hilberink, A., *Mechanical Behaviour of Lined Pipe. Chapter 6*, 2011, TU Delft. p. 105-210.
23. Meertens, B., *Experimenteel onderzoek naar het vermoeiingsgedrag van geschroefde buisverbindingen*, in *Mechanische constructie en productie*, Universiteit Gent: Gent. p. 115.
24. *Strain-Based Design of Pipelines*. 2003.
25. *Pipe Formulas*. Available from: www.engineeringtoolbox.com/pipe-formulas-d_1335.html.
26. *Calculate Section Properties of a Pipe Or Round HSS Section*. Available from: www.cecalc.com/SteelShapes/RoundSectionProperties.aspx.
27. Denys, R., *Pipeline Technology*, 2000, Gulf Professional Publishing.
28. Wong, B., *Plastic analysis and design of steel structures*. 1st ed. 2009, Amsterdam ; Boston: Butterworth-Heinemann. x, 246 p.
29. Yu, T.X. and L. Zhang, *Plastic bending*, in *Theory and Applications*, 1996, World Scientific.
30. Gresnigt, A.M. and R.J. Foeken. *Local Buckling of UOE and Seamless Steel Pipes*. in *Procedeeing of the 11th International Offshore and Polar Engineering Conference*. 2001. Stavanger, Norway.
31. Xue, L., *A unified expression for low cycle fatigue and extremely low cycle fatigue and its implication for monotonic loading.* International Journal of Fatigue, 2008. **30**(10-11): p. 1691-1698.
32. Focke, E.S. and J.T. Fokkema, *Reeling of Tight Tit Pipe*, Technische Universiteit Delft. p. 267.
33. Rossi, M., G.B. Broggiata, and S. Papalini, *Identification of Ductile Damage Parameters Using Digital Image Processing.*